Highly-Precise, Controllable Biaxial Deformation of 2-Dimensional Molybdenum Disulfide via Novel Micro-Gaussian Surfaces

By: Harrison Sinclair Shapiro

Abstract

Recently, research into two-dimensional materials has shifted from graphene to transition metal dichalcogenides (TMDs), especially monolayer molybdenum disulfide (MoS_2), a direct band gap semiconductor that shows potential for, amongst other applications, surpassing Moore's Law and revolutionizing foldable circuitry. Researchers have studied applying uniaxial strain to tune MoS_2's band gap, but permanent biaxial straining of TMD monolayers has never previously been achieved. In this study, novel micro-Gaussian surfaces (MGSs) have been created for permanent, precise biaxial deformation of two-dimensional MoS_2 films. These MGSs, produced using a customized photoresist reflow technique and reactive ion etching, have allowed for the first near-perfect draping of a two-dimensional TMD film onto a three-dimensional patterned substrate, as well as the first precise, permanent biaxial deformation of MoS_2. Raman analysis of MoS_2 draped over MGSs confirmed that MGSs modified the films' Raman shift and band gap. With further study, such surfaces have the potential to eventually tune electrical and optical properties of MoS_2 for numerous commercial applications, including replacing amorphous silicon in computer displays, as well as in high-sensitivity and broad-spectrum photodetectors.

Introduction

Early research into two-dimensional (2D) materials focused primarily on graphene, an allotrope of carbon that forms a 2D hexagonal lattice and serves as a suitable model for basic properties of 2D materials. However, graphene's lack of an electronic bandgap makes it unsuitable for use in electronic applications as a semiconductor, especially in microprocessors.[1] Recently, however, transition metal dichalcogenides (TMDs – inorganic compounds of the type MX_2, where M is a transition metal and X is either S, Se, Te, or Po), have emerged as a class of

atomically-thin materials with non-negligible, precisely-adjustable band gaps, which give TMDs incredible versatility for numerous applications that are currently impossible using graphene, silicon, or other three-dimensional (3D) semiconductors.[2] This study focuses on permanent biaxial deformation of the TMD MoS_2, a band gap tuning method that has not previously been studied. Novel micro-Gaussian surfaces, capable of inducing precise deformation at values between 1-5%, were produced with a heavily-customized photoresist reflow method. Using these substrates, the first near-perfect transfer of a 2D TMD film onto a 3D substrate was achieved, and band gap changes were detected in strained portions of transferred films.

MoS_2 is the most-studied 2D TMD due to its excellent optical and electronic properties, which give it the potential to miniaturize circuits beyond Moore's Law, create fully-foldable microcircuits, and replace existing silicon-based semiconductors for certain applications, especially in computer displays, flexible radio frequency identification tags, and low-power field effect transistors.[3] Bulk MoS_2 has a 1.2 electron-volt (eV) indirect band gap, while at the atomic limit, monolayer MoS_2 displays a 1.8 eV direct band gap. This direct band gap makes it superior to silicon (which has an indirect band gap) for next-generation nanoscale light production and detection devices, such as high-sensitivity photodetectors,[4] ultra-small light sources, and supercomputer technology.[5] MoS_2's electrical properties are similarly promising. It displays superior electron mobility compared to amorphous silicon, a common semiconductor, with around 200-500 cm^2/Vs and 30-114 cm^2/Vs (cm^2/Vs shows $\frac{\text{electron speed}}{\text{electric field strength}}$),[6] respectively, versus amorphous silicon's 1 cm^2/Vs.[7] Transistors made with atomically-thin MoS_2 show an on/off current ratio of 10^6-10^7, suitable for commercial applications.[8]

Despite MoS_2's numerous intriguing properties, producing few-layer samples reliably had historically been difficult. For many years, the primary production method was mechanical

exfoliation, which used tape to remove a few layers of MoS_2 from a larger crystal.[9] This method was incredibly flawed, though, requiring intense labor to produce regions between 10-100μm in size that contained varying numbers of MoS_2 layers, even within a single sample. However, in 2015, researchers developed a Metal Organic Chemical Vapor Deposition (MOCVD) process that reliably produced wafer-scale homogeneous films of monolayer MoS_2.[10] This MOCVD-grown MoS_2 displayed vastly superior electron mobility compared to exfoliated samples (1-2 orders of magnitude), making it far more promising for semiconductor applications.[11] More importantly, MoS_2 could be grown efficiently over an entire four-inch wafer, permitting large-scale production for research and commercial purposes.[12]

To optimize MoS_2 for semiconducting applications, researchers must determine how to precisely tune properties like band gap and optically-excited wavelength emission (Raman shift).[13] Theoretical and experimental studies have demonstrated that applying uniaxial strain to MoS_2 films can precisely adjust both of these properties in monolayer and few-layer MoS_2.[14] Biaxial strain, though, has barely been studied experimentally despite numerous theoretical calculations.[15] The intrinsic biaxial strain of CVD-grown MoS_2 has been examined, but such strain is neither tunable nor consistent between samples.[16] One experimental researcher has tested certain biaxial strain properties over a pressure membrane,[17] but such tests can only happen in a special chamber. However, no experimental studies exist on precisely, permanently biaxially straining monolayer MoS_2, as it would have to be deformed for practical applications.

No such experimental studies exist because nobody has previously permanently, biaxially deformed a 2D MoS_2 film. Uniaxial strain-induction methods, such as using a cantilever or deforming an MoS_2-polymer alloy,[18] do not work for biaxial deformation. However, the recent development of a vacuum technique for substrate transfer of MoS_2 now allows monolayer

stacking that can tune thickness with atomic precision, or reconfigure 2D MoS_2 into a 3D shape by transferring onto a pre-patterned substrate,[19] which studies in graphene have shown could induce fairly uniform strain lattices if done correctly.[20]

This study focuses on designing micro-Gaussian surfaces (MGSs), which have non-zero Gaussian curvature at all protruding points, to biaxially strain MoS_2 monolayers through stretching the 2D film onto the 3D surface. This MGS design is inspired by the smooth, periodically bumpy structure of Microlens Arrays (MLAs) used in optics. However, MLAs' dimensions, which are designed for optics, preclude them from inducing measurable strain in 2D films, while proportions that optimize strain make a surface useless for optics. Furthermore, the MoS_2 transfer method, as reported by Kang & Lee, et al., fails for MLAs. Thus, a customized MGS is needed that can biaxially deform MoS_2 precisely, while allowing for reliable, clean transfer of monolayer films. Creating these surfaces allows for the first-ever precision experimental studies of how permanent biaxial deformation affects MoS_2's optical properties.

Materials & Methods

The design of these strain-tunable MGSs is based on the square grid arrangement of spherical caps used in most commercial MLAs. Spherical caps function well for biaxial straining of 2D films because their smooth curvature distributes strain across the entire cap, rather than concentrating it in a highly-localized region (Similarly to why hemispheric bubbles form in pressure membrane tests).[21] Furthermore, this pattern can reliably be produced *en masse* through photoresist (PR) reflow – the formation of spherical caps via minimization of surface tension in melted polymer cylinders. Reflow of PR structures on Si and SiO_2 has been extensively studied as a method for producing MLAs.[22] Numerous variations of the protocol exist for different

optical applications, such as using special materials or creating biconvex lenses,[23] but a unique method has not previously been developed for production of strain-tunable MGSs.

To produce a 4-inch fused silica wafer patterned with correctly-sized PR columns, a standard photolithography procedure was followed (The graduate research assistant carried out photolithography using patterns of my design). The wafer was first washed to remove contaminants, then dehydrated by baking for ten minutes at 180°C. It was then coated with a uniform layer of positive AZ MiR 703 photoresist through spin coating at 3500 RPM for 45s, followed by a 60s soft-bake at 95°C to solidify the layer. To form the columns by selectively removing PR, the wafer was then inserted into a maskless aligner for photolithography (Heidelberg MLA150), and the locations of desired columns were exposed to 375nm UV light at a dosage of 105 mJ/cm^2 to make them insoluble in developer. After UV exposure, the wafer was hard-baked at 115°C for 60s, then developed with AZ 300MIF for 25s to dissolve unexposed regions of PR. After developing, it was rinsed thoroughly to remove any remaining particles.

Once wafers were patterned with PR cylinders, they were heated on a hot plate to induce PR reflow. Various times and temperatures between 130-200°C were investigated, and 15min at 200°C was discovered to be the optimal combination for MiR 703 PR. Profilometry with a Bruker Dektak XT-S profilometer was used to confirm that reflow successfully occurred.

To transfer the pattern of PR spherical caps onto fused silica, reactive ion etching (RIE) was performed on the patterned wafers using an Oxford Instruments Plasma-Pro NGP80. Depending on the desired depth of the caps, samples were etched for 90-105mins at 100W RF power with a recipe consisting of 25 standard cubic centimeters per minute (sccm) of CHF_3, 1.5-2.5sccm of O_2, and 22.5-23.5sccm of Ar, with the combined Ar and O_2 flows always adding to 25sccm. This was followed by a 125s O_2 plasma etch with 50sccm O_2 and 100W RF power to

clean the sample. Once removed from the etching machine, samples were washed to remove particles. Profilometry was repeated to ensure that the pattern conformed to a spherical cap profile. To confirm that MGSs were PR-free, some samples were removed from the RIE machine prior to the O_2 plasma etch, profiled, oxygen etched, and profiled again. The results of the two profiles were then compared.

MoS_2 substrate transfer was carried out on MOCVD-grown MoS_2 films using the stacking procedure developed by Kang and Lee et al.[24] 495K Poly(methyl methacrylate) (PMMA) was spin-coated onto as-grown MoS_2 samples for 30 seconds, then heated for five minutes at 180°C to increase uniformity of the PMMA layer. Thermal release tape (TRT) was then applied to the sample, followed by a 40s water vapor treatment to facilitate delamination of the MoS_2. The TRT was then peeled off the source wafer, placed into a vacuum stamping apparatus pre-heated to 150°C, evacuated to <200mTorr, and pressed onto the MGS for 5mins before removal from the vacuum. After 10mins post-transfer heating at 180°C to detach the thermal release tape from the PMMA/MoS_2, PMMA was removed by 6hrs of vacuum annealing at 350°C below 3×10^{-6} Torr. "In-air" stacking onto commercial MLAs followed a similar procedure, with a hole in the center of the TRT that suspended PMMA/MoS_2 and was slightly larger than the MLA. Instead of placing the TRT/PMMA/MoS_2 into the vacuum stamping apparatus, the hole was aligned over the MLA, and the surrounding TRT was cut away with a scalpel. PMMA removal was done with an identical annealing cycle.

Imaging of both bare MGSs and MoS_2-coated substrates was carried out a Zeiss Merlin scanning electron microscope (SEM, operated by the graduate research assistant) and optical microscopy (Olympus BX41). Raman and photoluminescence data and mapping were done with a Horiba LabRamHR Evolution confocal Raman microscope using a 533nm laser.

Theoretical induced strain levels (ε) of MGSs were calculated by modelling protrusions as spherical caps and comparing their surface area to the area of a 2D circle of equivalent radius with the following formula: $\varepsilon = \frac{(r^2+h^2)}{r^2}$, where r is the radius and h the height of protrusions. Conformance of profilometry data to spherical cap models was confirmed using a Wilcoxon signed-rank test (SRT) performed with XLSTAT in Microsoft Excel.

Results

This specialized fabrication method successfully produced MGSs capable of theoretically deforming MoS_2 by precise values between 1-5%, at roughly 1% intervals. All MGS samples were produced from identical reflowed wafers with PR cylinders of radius 10µm. Fig. 1 shows

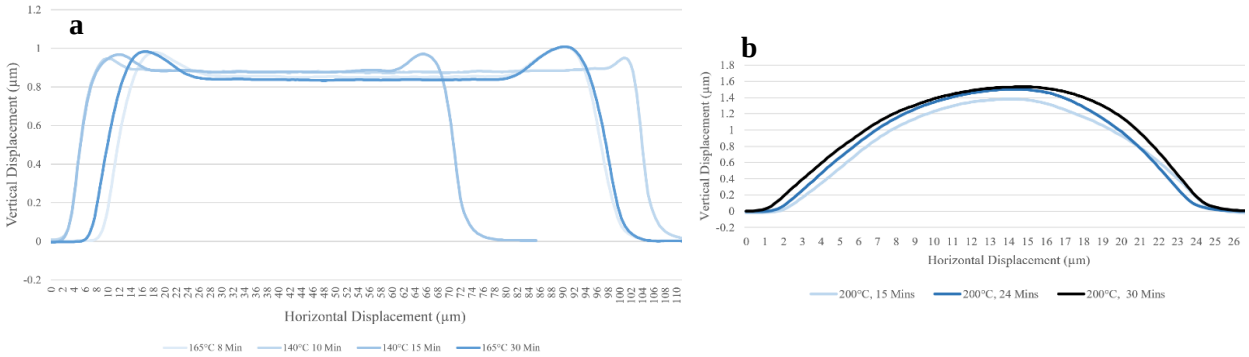

Figure 1: ***a.*** *Profiles of identical initial PR protrusions following attempted reflow at temperatures from 140°C-165°C for 8 to 30 minutes* ***b.*** *Profiles of identical initial PR protrusions following reflow at 200°C from 15 to 30 minutes.*

how reflow was minimal below 200°C, but there was little difference between samples heated for different times at 200°C.

Protrusion height, and thereby induced deformation, was varied by adjusting the O_2 flow in the RIE, with higher O_2 flows producing shorter protrusions, as this would increase the etch rate of PR without significantly changing that of silica. SEM imaging of MGSs revealed that reducing the O_2 flow increased the etching time needed due to the reduced PR etch speed. Fig. 2 shows SEM images of completely and incompletely etched protrusions, as well as a plot of

whether different recipe/time combinations were successful. As shown in Fig. 3, O_2 flows ranging from 1.5sccm to 3sccm produced protrusions between 2.3 µm and 1.5 µm tall.

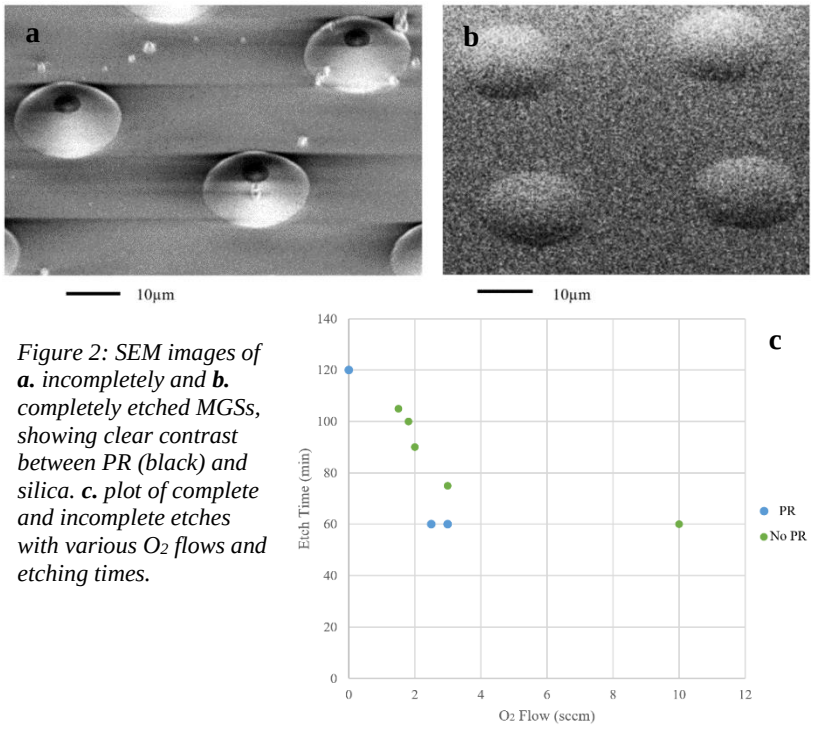

*Figure 2: SEM images of **a.** incompletely and **b.** completely etched MGSs, showing clear contrast between PR (black) and silica. **c.** plot of complete and incomplete etches with various O_2 flows and etching times.*

Post-etch MGSs almost perfectly fit a spherical cap model. A Wilcoxon RST of PR-free MGSs compared to ideal spherical caps of equal max height and radius gave p-values of <0.0001 for all PR-free MGSs (hypothesized difference = 0; 75-83 data points/MGS; n = 4 types of differently-etched MGSs). Since a strict p-value for a Wilcoxon RST is 0.01, this indicates that these MGSs are near-perfect spherical caps and can be accurately modeled as such. The theory behind reflow supports this, as melted PR should form a spherical cap shape to minimize surface tension.[25] Likewise, the anisotropic RIE should, in theory, maintain this pattern. This is consistent with the results of Daly et al., Di and Du, Rocha et al., and others.[26]

SEM imagery and profilometry of etched samples before and after a high-O_2 cleaning etch confirmed the absence of PR on MGSs used for MoS_2 transfer. Samples profiled before and after an

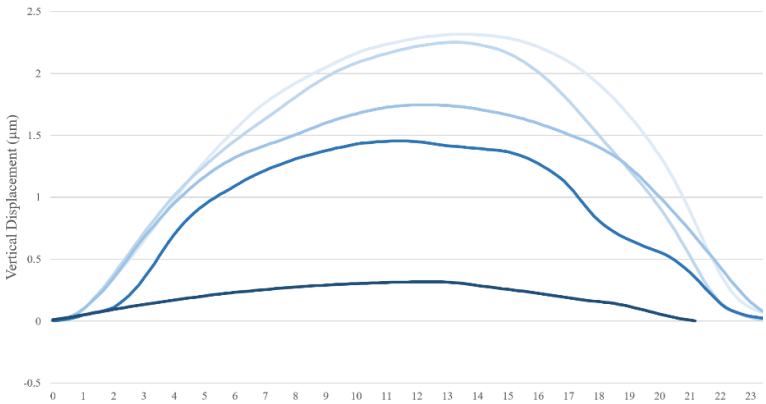

Figure 3: Profiles of MGS protrusions from identical initial samples after etching with various O_2 flows.

O_2 plasma etch showed no difference in protrusion profile between the two samplings. If PR were present, the high O_2 flow etch would have deformed the spherical cap pattern, and the post-etch profile would look different from the initial one. Fig. 2 shows SEM images of both a fully and a partially-etched MGS. As demonstrated by the partially-etched sample, which has a black ring of PR on the top of each protrusion, PR is clearly visible in SEM images. However, the fully-etched sample shows no black sections of PR, nor signs of particulate contamination.

Even though they induce near-zero amounts of strain, commercially-available MLAs are not suitable for MoS_2 film transfers. A commercial MLA does not work with Kang and Lee, et al.'s vacuum transfer technique because stamped TMD layers do not adhere to the substrate. The reason is as follows: for a transfer to be successful, there must be sufficient adhesion between the TMD film and the substrate prior to removal of the thermal release tape. Adhesion between silica and MoS_2 monolayers arises from Van der Waals (VDW) interactions, which are only significant when materials are nearly touching ($\leq$ 0.6nm apart). When MoS_2 monolayers are stamped onto flat substrates under vacuum, VDW adhesion occurs across the entire MoS_2-substrate contact area, anchoring the TMD film. However, when MoS_2 is stamped onto commercial MLAs, it only contacts only the tips of protrusions, which is insufficient for securing the film to the substrate (see Fig. 4). Thus, vacuum stacking onto commercial MLAs fails due to near-zero VDW

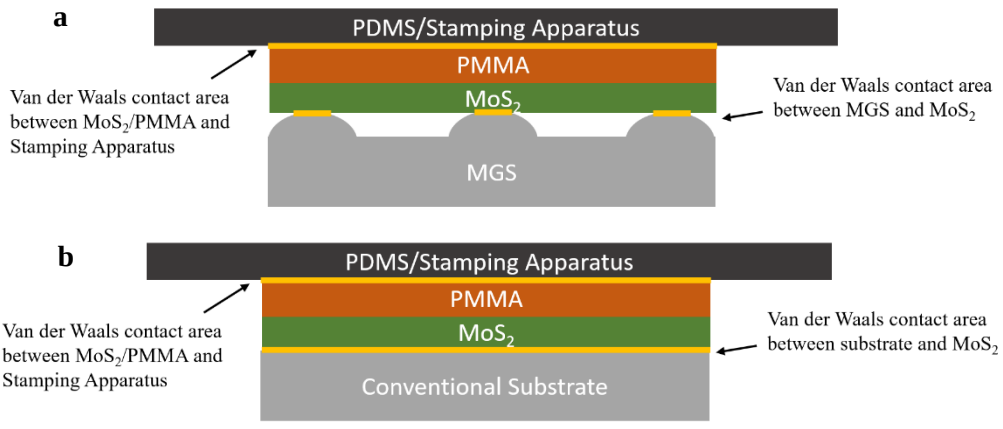

*Figure 4: Diagrams comparing relative Van der Waals (VdW) contact areas between MoS_2, transfer substrates, and the vacuum stacking apparatus for **a.** an MGS and **b.** a conventional substrate, showing the drastically different stamp/substrate contact area ratio when comparing flat substrates and MGSs.*

adhesion. To transfer MoS_2 onto a commercial MLA, an in-air stacking technique must be performed by hand, which eliminates the stamping apparatus and corresponding issues. As Kang at Lee, et al. have noted, though, in-air stacking creates far more defects than vacuum transfers.[27] Fig. 5 shows SEM imagery of a commercial MLA, with theoretical induced strain of 0.04%. Widespread wrinkling/tearing of the MoS_2 is visible, even at a relatively low magnification. Since these deformations are not tangential to protrusions, they are the result of transfer issues

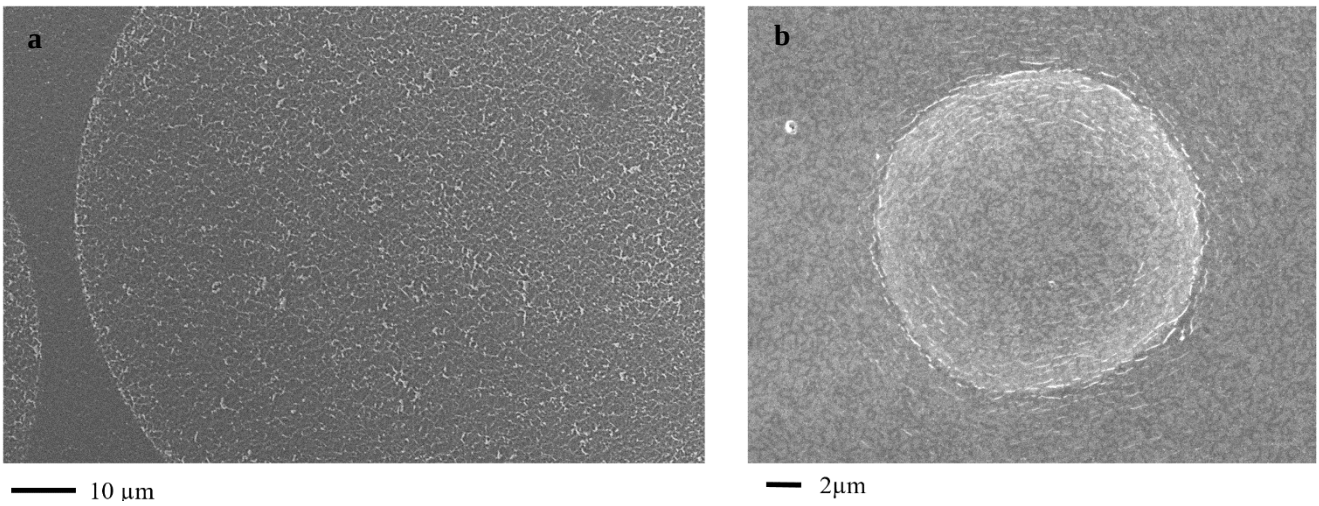

*Figure 5: SEM images of MoS_2 transferred **a.** via an in-air transfer technique onto a ThorLabs MLA150-5C and **b.** via vacuum stacking onto a purpose-built micro-Gaussian surface, showing vast reduction in wrinkling and elimination of tearing when comparing the MGS to the conventional MLA, especially when considering the higher magnification of the MGS image (in the higher-magnification MGS image, the light/dark pattern present throughout is monolayer MoS_2, not topographic defects).*

rather than induced strain, demonstrating how MLAs are poor substrates for MoS_2 transfer.

In comparison, the MGSs invented in this study permit vacuum transfer of MoS_2, vastly increasing the quality of transferred samples. Successful stamping was accomplished through creating a substrate with 2x2mm Gaussian regions surrounded by flat SiO_2 (see Fig. 6). The VDW adhesion between the MoS_2 monolayer and the flat portion of the substrate is sufficient to anchor the entire transferred sample, despite the lack of adhesion in Gaussian regions. Vacuum transfers result in far cleaner transfers onto MGSs compared to MLAs, despite the fact that MGSs induce far more strain, as shown in Fig. 5. While there is some wrinkling on the protrusions, wrinkles are few in number and tangential to the vertical slope of the MGS,

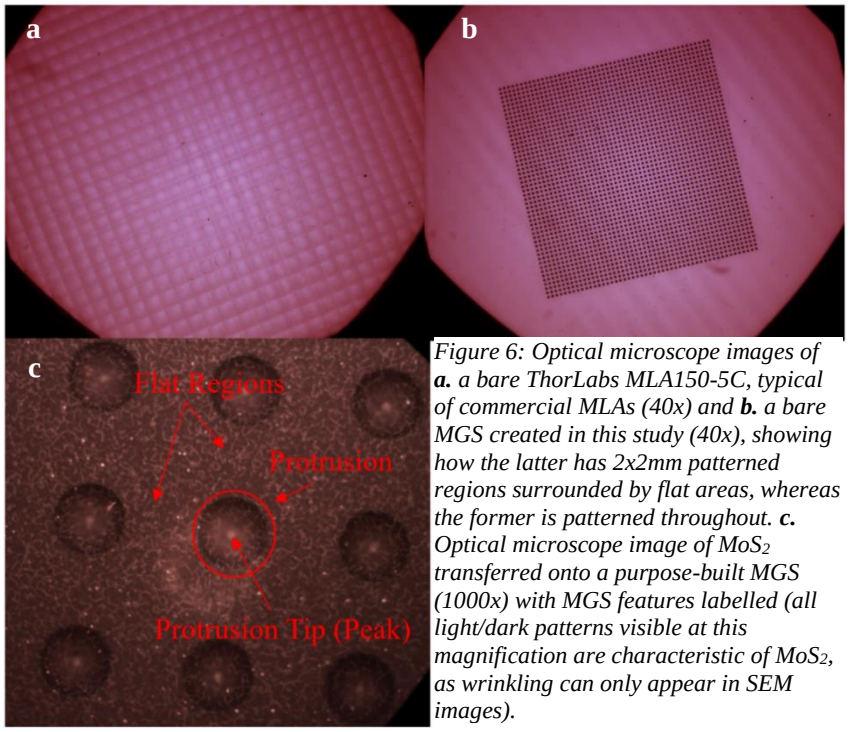

*Figure 6: Optical microscope images of **a.** a bare ThorLabs MLA150-5C, typical of commercial MLAs (40x) and **b.** a bare MGS created in this study (40x), showing how the latter has 2x2mm patterned regions surrounded by flat areas, whereas the former is patterned throughout. **c.** Optical microscope image of MoS_2 transferred onto a purpose-built MGS (1000x) with MGS features labelled (all light/dark patterns visible at this magnification are characteristic of MoS_2, as wrinkling can only appear in SEM images).*

indicating that they are strain-induced, rather than caused by transfer issues. This is supported by the lack of defects in the flat regions between protrusions.

Raman spectroscopy was used to confirm the successful transfer of monolayer MoS_2 onto manufactured MGSs. Sampling along the surface of MGSs using a ~1μm laser spot showed Raman shift peaks consistent with the $E_{2g}{}^1$ and A_{1g} modes of monolayer MoS_2, which occur around 384 cm^{-1} and 403 cm^{-1}, respectively.[28] The presence of such peaks confirms that a monolayer of MoS_2 was completely transferred onto the MGSs. Since SEM imaging showed evidence of MoS_2 wrinkling near the edges of protrusions, Raman spectroscopy was used to confirm that the MoS_2 surface was continuous and not torn. If there had been significant tearing, some locations would not have returned these double peaks. However, repeated Raman sampling along the edges of multiple MGSs' protrusions consistently returned the $E_{2g}{}^1$ and A_{1g} peaks. The precision of this method for examining the presence of monolayer MoS_2 was confirmed using control samples and known defective transfers. Raman spectroscopy of these samples displayed no $E_{2g}{}^1$ or A_{1g} peaks when the laser spot was focused on tears or MoS_2-free regions, corroborating SEM images.

Raman spectroscopy of protrusions on successfully-transferred samples displayed a slight change in Raman shift on protrusions compared to nearby flat regions. Raman peaks taken at the top of protrusions generally yielded Raman shifts of around $1cm^{-1}$ in the $E_{2g}{}^{1}$ peak when comparing protrusion tips to neighboring flat regions. Edge regions of protrusions tended to display shifts with values between these two. Analysis of the MoS_2's band gap using photoluminescence yielded a similar result, with shifts of ~20meV best shown by Raman mapping in Fig. 7, which demonstrates a marked overall reduction in MoS_2's band gap for MoS_2 over the protrusion, compared to neighboring flat regions.

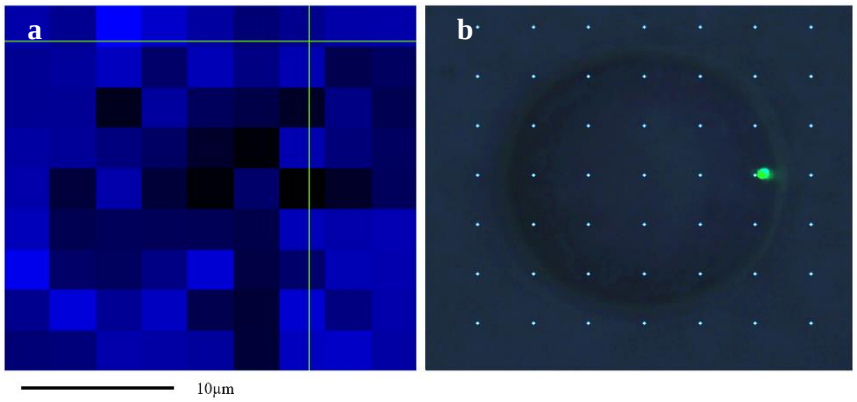

Figure 7: ***a.*** *9x9 Raman map of the size of monolayer MoS_2's bandgap across the surface of an MGS protrusion, with darker shades representing a narrower bandgap.* ***b.*** *Optical microscope image overlaid with sampling locations for this Raman map.*

Discussion

Despite abundant literature on the PR reflow method of producing MLAs, the protocols prescribed by other studies required significant modification to produce MGSs. The temperature at which PR reflow occurred was not consistent with other research. Literature reported that PR reflow should occur at 130-140°C,[29] but significant reflow of photoresist cylinders in this experiment did not occur below 200°C. Although MiR 703 PR was not used in other literature studies, this extremely high reflow point conflicts with technical documentation.[30] One possibility for why this occurred was the relatively high ratio of PR cylinder height to diameter, which was greater than in other studies.[31] Another is that a "hard bake" was incorporated after developing the PR, something not typically done in reflow studies, where the "hard bake" is

replaced by the reflow itself. However, an advantage of adding this step is that the PR cylinders display excellent longevity in storage, even at atmospheric pressure with frequent light exposure. The reactive ion etch process also had to be heavily modified from expected protocol. In most cases, a typical fused silica etch (fused silica should not be confused with thermally-oxidized SiO_2, which is far less resilient) with CHF_3 and Ar should etch fused silica at around 300-400Å/min with 3:1 PR to SiO_2 selectivity (an etch rate of 900-1200Å/min for PR).[32] However, experimentally-determined etch rates in this study showed that a pure CHF_3/Ar (25sccm each) etch actually etched fused SiO_2 at around 135Å/min with a 1:3 PR to SiO_2 selectivity (an etch rate of 45Å/min for PR). A possible explanation for this exceptionally-low PR etch rate is that, in most normal applications, PR is never heated to 200°C before etching. When heated to melting temperatures and allowed to cool, some polymers exhibit extensive crosslinking between individual polymer chains. Known as "thermosetting" in industrial applications, this creates a crosslinked material that is far more resistant to melting and etching than the original.[33] Besides the slower-than-expected etching of PR, a possibility for the slow etching of SiO_2 is that the fused silica used by other researchers may have been of lesser quality. Since SiO_2 is available from a wide variety of sources for vastly differing purposes, there could easily have been wide discrepancies between samples used by different researchers.

Although the MGSs produced in this study share a similar layout and production method with standard MLAs, they are unique because they are designed with induced strain in mind, rather than optical properties. The MGSs' focal lengths of around 40μm are useless for optical applications, as MLAs generally have a focal length of several hundred microns to a few millimeters.[34] Since MLAs are usually used for focusing light on CMOS photodetectors, this focal length would require the detector to be just 40μm behind the protrusion, which is entirely

unfeasible for practical applications. The small radius of protrusions, combined with the relatively high protrusion height to diameter ratio (~0.1 for MGSs, compared to ~0.01 for commercial MLAs), are what make MGS protrusions properly sized for straining films by 1-5%. However, these same dimensions are also what give the MGSs poor optical properties. Conversely, the proportions of commercial MLAs produce excellent optical properties, but negligible induced strain. The mutual exclusivity of optical and strain induction properties explains why, despite decades of research into MLA fabrication, no MLAs exist that are suitable for straining 2D materials.

The successful transfer of MoS_2 monolayers onto MGSs also represents the first near-perfect draping of a 2D TMD film onto a patterned 3D substrate. SEM imaging reveals few defects in the film transfer, a finding confirmed by Raman spectroscopy. In a 9x9 Raman mapping of an MGS protrusion and surrounding flat regions, all 81 data points returned a direct band gap, demonstrating the presence of monolayer MoS_2. Raman sampling along various parts of different MGS samples returned similar results, confirming that the MoS_2 layer was complete and monolayer throughout the patterned substrate, a first-ever achievement for monolayer TMDs. Although graphene has previously been draped over silica nanopillars,[35] researchers were unable to get it to conform to the

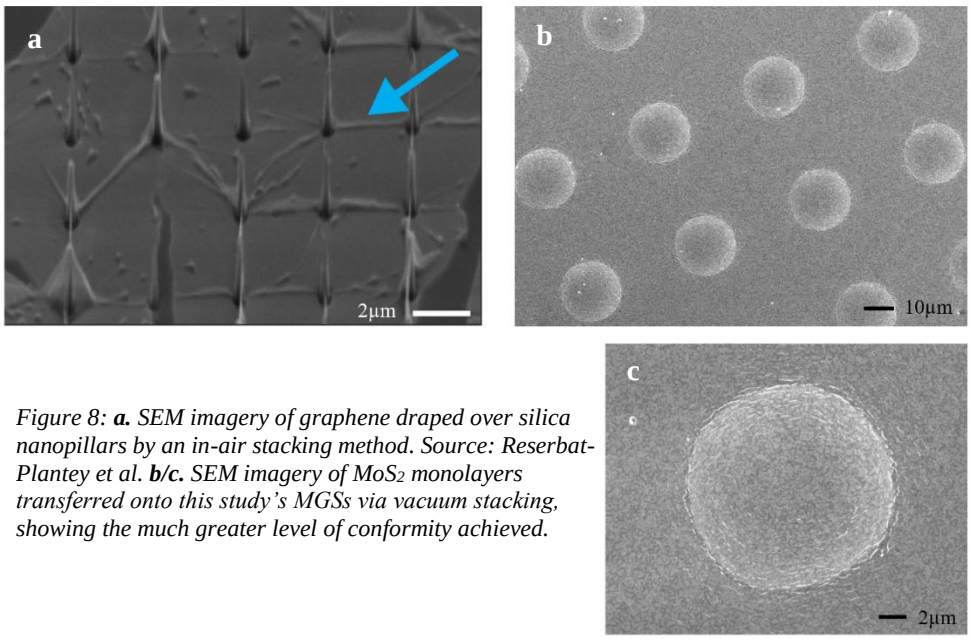

Figure 8: ***a.*** *SEM imagery of graphene draped over silica nanopillars by an in-air stacking method. Source: Reserbat-Plantey et al.* ***b/c.*** *SEM imagery of MoS_2 monolayers transferred onto this study's MGSs via vacuum stacking, showing the much greater level of conformity achieved.*

substrate's topography. There was widespread wrinkling and tearing, as well as frequent suspension of the graphene film above the substrate, creating an intermediate air pocket.[36] In Fig. 8, SEM imagery of Reserbat-Plantey et al.'s graphene-over-silica is contrasted with an SEM image of monolayer MoS_2 draped over an MGS from this study. The development of a smooth, micro-Gaussian substrate, as well as use of a vacuum stacking method for TMD monolayer transfer, has enabled reduction of these defects.

Raman analysis of MoS_2 draped over MGS protrusions supports the hypothesis that the MGSs would induce strain in transferred MoS_2. Conforming a flat TMD sheet to an uneven substrate forces the original film to expand as it covers the 3D topographic surface, inducing strain. In the case of graphene draped over silica nanopillars, a strain lattice effect was detected through Raman mapping of the transferred film.[37] Likewise, in this study, a clear change in Raman shift was observed for MoS_2 on MGS protrusions compared to nearby flat regions (see Fig. 7). In a Raman mapping of photoluminescence in an MoS_2-covered MGS protrusion (theoretical $\varepsilon = 4.8\%$), there was a ~20meV decrease in the MoS_2's band gap compared to a nearby flat area. However, literature suggests that this decrease should be around 350-500meV at 4.8% applied strain.[38] Similarly, an analysis of the $E_{2g}{}^1$ peak of MoS_2 draped onto an MGS (theoretical $\varepsilon = 2.1\%$) showed a decrease of ~1cm^{-1} when comparing a protrusion tip to a neighboring flat region. Once again, literature suggested that a decrease of around 3-4cm^{-1} in the $E_{2g}{}^1$ peak would occur under 2.1% applied strain.[39] A possible explanation for this phenomenon is that, since stamped MoS_2 films contacted the tops of protrusions first, then stretched to conform to the patterned surface, strain became evenly distributed throughout the MGS. Strain lattices observed in strained graphene also displayed this property.[40] The effects of releasing MOCVD-grown MoS_2's intrinsic biaxial strain ($\varepsilon \approx 1.24\%$) during transfer could also affect the

final distribution of applied strain.[41] Another possibility is that the MoS_2 film became torn along the edges of protrusions, causing it to elastically rebound to a zero-strain state. However, this is unlikely given that repeated SEM imaging, precision Raman mapping of protrusions, and thorough random Raman sampling suggest a continuous monolayer of MoS_2.

Conclusions & Future Work

Although this study's MGSs were produced using a variation of the existing photoresist reflow process, they are novel substrates in that: they have vastly greater height to diameter ratios than any existing MLA, allowing them deform films by 1-5%; they are the first surface to permanently biaxially deform a 2D film at precise intervals (of ~1%); and they are compatible with MoS_2 vacuum stamping, allowing for the first-ever near-perfect draping of a 2D TMD film over a 3D topographic substrate. While MLAs have existed for decades, the size proportions required to optimize optical properties preclude the ability to induce meaningful amounts of strain, and vice-versa, so no appropriately-proportioned surfaces previously existed. Although some wrinkling is present in transferred MoS_2 monolayers, the conformance of MoS_2 monolayers to MGS surfaces eclipses the accuracy that previous researchers have achieved with graphene.[42] Extensive Raman analysis and SEM imaging have confirmed the continuity of the transferred films across the surfaces of MGSs, showing that these transfers were successful.

Now that 2D TMD films can reliably be transferred onto MGSs, the properties of these deformed films can be thoroughly investigated. Specifically, researchers will be able to examine the effects of conforming a TMD monolayer to a 3D substrate. Raman data shows that, as expected, there is a reduction in the $E_{2g}{}^1$ peak location and band gap of monolayer MoS_2 when comparing protrusion tips with nearby flat regions, consistent with applied strain. However, the magnitude of these shifts was far less than literature would suggest for the MGSs' theoretical

induced strain. A possible cause is that, although strain is somewhat localized at protrusions (as shown by the Raman mapping), much of it is evenly distributed throughout the entire surface. Although this is unexpected, the commercial implications could be even greater than for highly-localized strain structures, as an entire transferred MoS_2 film could be engineered with near-uniform electro-optical properties. Further study is needed to confirm that this is the cause of these smaller-than-expected shifts, though. One useful experiment would be a first-principles study comparing Van der Waals TMD-substrate interactions and in-plane restorative forces in MoS_2 to calculate the maximum possible amount of permanently-inducible biaxial strain.

Once these electro-optical shifts are understood, simple devices, such as field-effect transistors, should be fabricated using MoS_2 draped over an MGS. This will allow for testing of a common commercial transistor made with biaxially-strained MoS_2. Such study could allow MGS substrates with transferred MoS_2 to become a platform for nanoscale optical devices, including next-generation photodetectors,[43] high-density vertically-stacked integrated circuits,[44] and ultra-small light sources.[45]

---

[1] Hee Sung Lee, et al., "MoS2 Nanosheet Phototransistors with Thickness-Modulated Optical Energy Gap," *Nano Letters* 12, no. 7 (2012): 3695-3700; Dattatray Late, et al., "Hysteresis in Single-Layer MoS2 Field Effect Transistors," ACS Nano 6, no. 6 (2012): 5635-5641; Hiram J. Conley, et al., "Bandgap Engineering of Strained Monolayer and Bilayer MoS2," *Nano Letters* 13, no. 8 (2013): 3626-3630; Hsiao-Yu Chang, et al., "High-Performance, Highly Bendable MoS2 Transistors with High-K Dielectrics for Flexible Low-Power Systems," ACS Nano 7, no. 6 (2013): 5446-5452.
[2] Wang, et al.; Late, et al.; Chang, et al.
[3] Wang, et al.; "Membrane-Based Electronics: Foldable & Adaptable Integrated Circuits: A DoD Multidisciplinary University Research Initiative," *Cornell University*, 2015, http://2dmuri.chem.cornell.edu/about/; Late, et al.
[4] Woong Choi, et al., "High-Detectivity Multilayer MoS2 Phototransistors with Spectral Response from Ultraviolet to Infrared," *Advanced Materials* 24, no. 43 (2012): 5832-5836; Oriol Lopez-Sanchez, et al., "Ultrasensitive photodetectors based on monolayer MoS2," *Nature Nanotechnology* 8, no. 7 (2013): 497-501; Wenyi Wang, et al., "Hot Electron-Based Near-Infrared Photodetection Using Bilayer MoS2," *Nano Letters* 15, no. 11 (2015): 7440-7444.
[5] Andrea Splendiani, et al., "Emerging Photoluminescence in Monolayer MoS2," *Nano Letters* 10, no. 4 (2010): 1271-1275; Wei Gao, et al., "Localized and Continuous Tuning of Monolayer MoS2 Photoluminescence Using a Single Shape-Controlled Ag Nanoantenna," *Advanced Materials (Deerfield Beach, Fla.)* 28, no. 4 (2016): 701-706.
[6] Branimir Radisavljevic and Andras Kis, "Mobility engineering and a metal-insulator transition in monolayer MoS2," *Nature Materials* 12, no. 9 (2013): 815-820; Kibum Kang and Saien Xie, et al., "High-mobility three-atom-thick semiconducting films with wafer-scale homogeneity," *Nature* 520, no. 7549 (2015): 656-660.
[7] Amy Turner, "Process and Performance of a-Si and poly-Si TFTs on Plastic." (Master's research, Cornell University, 2006), http://people.ccmr.cornell.edu/~cober/mse542/page2/files/AmyTurnerTFT%20on%20Plastic.pdf.
[8] Lee, et al.
[9] Hai Li, et al. "Preparation and Applications of Mechanically Exfoliated Single-Layer and Multi-layer MoS2 and WSe2 Nanosheets," *Accounts of Chemical Research* 47, no. 4 (2014): 1067-1075.

[10] Kang and Xie, et al.
[11] Ibid. Radisavljevic and Kis, 3.
[12] Kang and Xie, et al.
[13] Priya Johari and Vivek B. Shenoy, "Tuning the Electronic Properties of Semiconducting Transition Metal Dichalcogenides by Applying Mechanical Strains," *ACS Nano* 6, no. 6 (2012): 5449-5456; Conley, et al.
[14] Johari and Shenoy; Ning Lu, et al., "MoS2/MX2 heterobilayers: bandgap engineering via tensile strain or external electrical field," *Nanoscale* 6, no. 5 (2014): 2879-2886; Conley, et al.; C. Rice, et al, "Raman-scattering measurements and first-principles calculations of strain-induced phonon shifts in monolayer MoS2," *Physical Review B* 87, no. 8 (2013); Yanlong Wang, et al., "Raman spectroscopy study of lattice vibration and crystallographic orientation of monolayer MoS2 under uniaxial strain," *Small (Weinheim An Der Bergstrasse, Germany)* 9, no. 17 (2013): 2857-2861; Keliang He, et al., "Experimental Demonstration of Continuous Electronic Structure Tuning via Strain in Atomically Thin MoS2," *Nano Letters* 13, no. 6 (2013): 2931-2936.
[15] Seyed M. Tabatabaei, et al., "A first-principles study on the effect of biaxial strain on the ultimate performance of monolayer MoS2-based double gate field effect transistor," *Journal of Applied Physics* 113, no. 16 (2013); Peng Tao, et al., "Strain-induced magnetism in MoS2 monolayer with defects," *Journal of Applied Physics* 115, no. 5 (2014); Won Seok Yun, et al., "Thickness and strain effects on electronic structures of transition metal dichalcogenides: 2H-MX2 semiconductors (M = Mo, W; X = S, Se, Te)," *Physical Review B: Condensed Matter & Materials Physics* 85, no. 4 (2012): 1-5.
[16] Amber McCreary, et al., "Effects of Uniaxial and Biaxial Strain on Few-Layered Terrace Structures of MoS_2 Grown by Vapor Transport," *ACS Nano* 10, no. 3 (2016): 3186-3197.
[17] David Lloyd, et al., "Band Gap Engineering with Ultralarge Biaxial Strains in Suspended Monolayer MoS2," *Nano Letters* 16, no. 9 (2016): 5836-5841; David Lloyd, et al., "Adhesion, Stiffness, and Instability in Atomically Thin MoS2 Bubbles," *Nano Letters* (2017).
[18] He, et al.; Wang, et al., "Raman spectroscopy study."
[19] Kibum Kang and Kan-Heng Lee, et al., "Layer-by-Layer Assembly of Two-Dimensional Materials into Wafer-Scale Heterostructures," (in press, *Nature*, 2017).
[20] Antoine Reserbat-Plantey, et al., "Strain Superlattices and Macroscale Suspension of Graphene Induced by Corrugated Substrates," *Nano Letters* 14, no. 9 (2014): 5044-5051.
[21] Lloyd, et al., "Band Gap Engineering"; Lloyd, et al., "Adhesion, Stiffness, and Instability."
[22] Si Di and Ru-xu Du, "The controlling of microlens contour by adjusting developing time in the thermal reflow method," *Proceedings of SPIE – The International Society for Optical Engineering* 7381, (2009): 73811D; R.P. Rocha, et al., "Microlenses Array Made with AZ4562 Photoresist for Stereoscopic Acquisition," *Procedia Engineering* 47, no. 26 (2012): 619-622; D. Daly, et al., "The Manufacture of Microlenses by Melting Photoresist," *Measurement Science and Technology* 1, no. 8 (1990): 759-766; Feidhlim T. O'Neill, and John T. Sheridan, "Photoresist reflow method of microlens production Part I: Background and experiments," *Optik - International Journal for Light and Electron Optics* 113, (2002): 391-404; Zoran D. Popovic, Robert A. Sprague, and G.A. Neville Connell, "Technique for Monolithic Fabrication of Microlens Arrays," *Applied Optics* 27, no. 7 (1988): 1281-1284.
[23] O'Neill and Sheridan.
[24] Kang and Lee, et al.
[25] Popovic, et al.; Daly, et al.
[26] Di and Du; Rocha, et al; Daly, et al.; O'Neill and Sheridan; Popovic, et al.
[27] Kang and Lee, et al.
[28] Wang, et al., "Raman spectroscopy study."
[29] Di and Du; Popovic, et al.; Rocha, et al.; "Reflow of Photoresist," *Microchemicals GmbH*. November 7, 2013, http://www.microchemicals.com/technical_information/reflow_photoresist.pdf.
[30] "Reflow of Photoresist," *Microchemicals GmbH*.
[31] O'Neill and Sheridan; Marco Severi and Patrick L. Mottier, "Etching selectivity control during resist pattern transfer into silica for the fabrication of microlenses with reduced spherical aberrations," *Optical Engineering* 38, no. 1 (1999): 146-150.
[32] "Application Notes: Plasma Etching of Silicon Nitride and Silicon Dioxide," *University of Wisconsin – Madison*, September 24, 1992, https://wcam.engr.wisc.edu/Public/Reference/PlasmaEtch/SiO2%20and%20Si 3N4%20RIE%20recipes.pdf; Meredith Metzler, "Reactive Ion Etch (RIE) of Silicon Dioxide (SiO2) with Trifluoromethane and Oxygen (CHF3/O2)," *University of Pennsylvania*, May 7, 2016, http://repository.upenn.edu/cgi/viewcontent.cgi?article=1038&context=scn_tooldata; Alan Selewa, "Fused Silica (glass) Etch," *University of Chicago*, December 3, 2015, https://uchicago.app.box.com/s/nfnu0qwd0dcmxbzp95meku3w7180m6tk.
[33] Jean-Pierre Pascault, et al., *Thermosetting Polymers* (Boca Raton, FL: CRC Press, 2002); Dodiuk Hanna and Sydney H. Goodman, *Handbook of Thermoset Plastics* (Burlington: Elsevier Science, 2013).
[34] Hsin-Ta Hsieh, et al., "Design and fabrication of long focal length microlens arrays," *Optics Communications* 284, (2011): 5225-5230; "Microlens Arrays," *Edmund Optics*, https://www.edmundoptics.com/optics/optical-lenses/specialty-lenses/Microlens-Arrays/; "Microlens Arrays," *SUSS MicroOptics SA*, http://www.amstechnologies.com/fileadmin/ams media/downloads/2067_SMO_catalog.pdf; "Microlens Arrays," *ThorLabs*, https://www.thorlabs.com/newgrouppage9.cfm?objectgroup_id=2861.
[35] Reserbat-Plantey, et al.
[36] Ibid.
[37] Ibid.

[38] Johari and Shenoy; Tao, et al.; Lloyd, et al., "Band Gap Engineering"; He, et al.
[39] Wang, et al., "Raman spectroscopy study"; Conley, et al.; Rice, et al.
[40] Reserbat-Plantey, et al.
[41] McCreary, et al.; Matin Amani, et al., "Growth-substrate induced performance degradation in chemically synthesized monolayer MoS2 field effect transistors," *Applied Physics Letters* 104, no. 20 (2014).
[42] Reserbat-Plantey, et al.
[43] Choi, et al.; Lopez-Sanchez, et al.; Wang, et al.
[44] Kang and Xie, et al.
[45] Gao, et al.

References

Amani, Matin, et al. “Growth-substrate induced performance degradation in chemically synthesized monolayer MoS2 field effect transistors.” *Applied Physics Letters* 104, no. 20 (2014).

“Application Notes: Plasma Etching of Silicon Nitride and Silicon Dioxide.” *University of Wisconsin – Madison*. September 24, 1992. https://wcam.engr.wisc.edu/Public/Reference/PlasmaEtch/SiO2%20and%20Si3N4%20RIE%20recipes.pdf.

Chang, Hsiao-Yu, et al. “High-Performance, Highly Bendable MoS2 Transistors with High-K Dielectrics for Flexible Low-Power Systems.” ACS Nano 7, no. 6 (2013): 5446-5452.

Choi, Woong, et al. “High-Detectivity Multilayer MoS2 Phototransistors with Spectral Response from Ultraviolet to Infrared.” *Advanced Materials* 24, no. 43 (2012): 5832-5836.

Conley, Hiram J., et al. “Bandgap Engineering of Strained Monolayer and Bilayer MoS2.” *Nano Letters* 13, no. 8 (2013): 3626-3630.

Daly, D, et al. “The Manufacture of Microlenses by Melting Photoresist.” *Measurement Science and Technology* 1, no. 8 (1990): 759-766.

Di, Si, and Ru-xu Du. “The controlling of microlens contour by adjusting developing time in the thermal reflow method.” *Proceedings of SPIE – The International Society for Optical Engineering* 7381, (2009): 73811D.

Gao, Wei, et al. “Localized and Continuous Tuning of Monolayer MoS2 Photoluminescence Using a Single Shape-Controlled Ag Nanoantenna.” *Advanced Materials (Deerfield Beach, Fla.)* 28, no. 4 (2016): 701-706.

Hanna, Dodiuk, and Sydney H. Goodman. *Handbook of Thermoset Plastics*. Burlington: Elsevier Science, 2013.

He, Keliang, et al. “Experimental Demonstration of Continuous Electronic Structure Tuning via Strain in Atomically Thin MoS2.” *Nano Letters* 13, no. 6 (2013): 2931-2936.

Hsieh, Hsin-Ta, et al. “Design and fabrication of long focal length microlens arrays.” *Optics Communications* 284, (2011): 5225-5230.

Johari, Priya, and Vivek B. Shenoy. “Tuning the Electronic Properties of Semiconducting Transition Metal Dichalcogenides by Applying Mechanical Strains.” *ACS Nano* 6, no. 6 (2012): 5449-5456.

Kang, Kibum and Kan-Heng Lee, et al. “Layer-by-Layer Assembly of Two-Dimensional Materials into Wafer-Scale Heterostructures.” In press, *Nature*, 2017.

Kang, Kibum and Saien Xie, et al. “High-mobility three-atom-thick semiconducting films with wafer-scale homogeneity.” *Nature* 520, no. 7549 (2015): 656-660.

Late, Dattatray, et al. “Hysteresis in Single-Layer MoS2 Field Effect Transistors.” ACS Nano 6, no. 6 (2012): 5635-5641.

Lee, Hee Sung, et al. “MoS2 Nanosheet Phototransistors with Thickness-Modulated Optical Energy Gap.” *Nano Letters* 12, no. 7 (2012): 3695-3700.

Li, Hai, et al. “Preparation and Applications of Mechanically Exfoliated Single-Layer and Multi-layer MoS2 and WSe2 Nanosheets.” *Accounts of Chemical Research* 47, no. 4 (2014): 1067-1075.

Lloyd, David, et al. “Adhesion, Stiffness, and Instability in Atomically Thin MoS2 Bubbles.” *Nano Letters* (2017).

Lloyd, David, et al. “Band Gap Engineering with Ultralarge Biaxial Strains in Suspended Monolayer MoS2.” *Nano Letters* 16, no. 9 (2016): 5836-5841.

Lopez-Sanchez, Oriol, et al. “Ultrasensitive photodetectors based on monolayer MoS2.” *Nature Nanotechnology* 8, no. 7 (2013): 497-501.

Lu, Ning, et al. “MoS2/MX2 heterobilayers: bandgap engineering via tensile strain or external electrical field.” *Nanoscale* 6, no. 5 (2014): 2879-2886.

McCreary, Amber, et al. “Effects of Uniaxial and Biaxial Strain on Few-Layered Terrace Structures of MoS_2 Grown by Vapor Transport.” *ACS Nano* 10, no. 3 (2016): 3186-3197.

“Membrane-Based Electronics: Foldable & Adaptable Integrated Circuits: A DoD Multidisciplinary University Research Initiative.” *Cornell University*. 2015. http://2dmuri.chem.cornell.edu/about/.

Metzler, Meredith. “Reactive Ion Etch (RIE) of Silicon Dioxide (SiO2) with Trifluoromethane and Oxygen (CHF3/O2).” *University of Pennsylvania*. May 7, 2016. http://repository.upenn.edu/cgi/viewcontent.cgi?article=1038&context=scn_tooldata.

“Microlens Arrays.” *Edmund Optics*. https://www.edmundoptics.com/optics/optical-lenses/specialty-lenses/Microlens-Arrays/.

“Microlens Arrays.” *SUSS MicroOptics SA.* http://www.amstechnologies.com/fileadmin/amsmedia/downloads/2067_SMO_catalog.pdf.

“Microlens Arrays.” *ThorLabs*. https://www.thorlabs.com/newgrouppage9.cfm?objectgroup_id=2861.

O’Neill, Feidhlim T., and John T. Sheridan. “Photoresist reflow method of microlens production Part I: Background and experiments.” *Optik - International Journal for Light and Electron Optics* 113, (2002): 391-404.

Pascault, Jean-Pierre, et al. *Thermosetting Polymers*. Boca Raton, FL: CRC Press, 2002.

Popovic, Zoran D., Robert A. Sprague, and G.A. Neville Connell. “Technique for Monolithic Fabrication of Microlens Arrays.” *Applied Optics* 27, no. 7 (1988): 1281-1284.

Radisavljevic, Branimir, and Andras Kis. “Mobility engineering and a metal-insulator transition in monolayer MoS2.” *Nature Materials* 12, no. 9 (2013): 815-820.

“Reflow of Photoresist.” *Microchemicals GmbH*. November 7, 2013. http://www.microchemicals.com/technical_information/reflow_photoresist.pdf.

Reserbat-Plantey, Antoine, et al. “Strain Superlattices and Macroscale Suspension of Graphene Induced by Corrugated Substrates.” *Nano Letters* 14, no. 9 (2014): 5044-5051.

Rice, C., et al. “Raman-scattering measurements and first-principles calculations of strain-induced phonon shifts in monolayer MoS2.” *Physical Review B* 87, no. 8 (2013).

Rocha, R.P., et al. “Microlenses Array Made with AZ4562 Photoresist for Stereoscopic Acquisition.” *Procedia Engineering* 47, no. 26 (2012): 619-622.

Selewa, Alan. “Fused Silica (glass) Etch.” *University of Chicago*. December 3, 2015. https://uchicago.app.box.com/s/nfnu0qwd0dcmxbzp95meku3w7180m6tk.

Severi, Marco, and Patrick L. Mottier. “Etching selectivity control during resist pattern transfer into silica for the fabrication of microlenses with reduced spherical aberrations.” *Optical Engineering* 38, no. 1 (1999): 146-150.

Splendiani, Andrea, et al. “Emerging Photoluminescence in Monolayer MoS2.” *Nano Letters* 10, no. 4 (2010): 1271-1275.

Tabatabaei, Seyed M., et al. “A first-principles study on the effect of biaxial strain on the ultimate performance of monolayer MoS2-based double gate field effect transistor.” *Journal of Applied Physics* 113, no. 16 (2013).

Tao, Peng, et al. “Strain-induced magnetism in MoS2 monolayer with defects.” *Journal of Applied Physics* 115, no. 5 (2014).

Turner, Amy. “Process and Performance of a-Si and poly-Si TFTs on Plastic.” Master’s research, Cornell University, 2006. http://people.ccmr.cornell.edu/~cober/mse542/page2/files /AmyTurnerTFT%20on%20Plastic.pdf.

Wang, Han, et al. “Integrated Circuits Based on Bilayer MoS2 Transistors.” Nano Letters 12, no. 9 (2012): 4674-4680.

Wang, Wenyi, et al. “Hot Electron-Based Near-Infrared Photodetection Using Bilayer MoS2.” *Nano Letters* 15, no. 11 (2015): 7440-7444.

Wang, Yanlong, et al. “Raman spectroscopy study of lattice vibration and crystallographic orientation of monolayer MoS2 under uniaxial strain.” *Small (Weinheim An Der Bergstrasse, Germany)* 9, no. 17 (2013): 2857-2861.

Yun, Won Seok, et al. “Thickness and strain effects on electronic structures of transition metal dichalcogenides: 2H-MX2 semiconductors (M = Mo, W; X = S, Se, Te).” *Physical Review B: Condensed Matter & Materials Physics* 85, no. 4 (2012): 1-5.